

The Structure and Dynamic Properties of Nitrile-Butadiene Rubber/Poly(vinyl chloride)/Hindered Phenol Crosslinked Composites

Ping Xiang,¹ Xiu-Ying Zhao,¹ Da-Ling Xiao,² Yong-Lai Lu,² Li-Qun Zhang^{1,2}

¹The Key Laboratory of Beijing City on Preparation and Processing of Novel Polymer Materials, Beijing University of Chemical Technology, Beijing 100029, China

²The Key Laboratory for Nano-materials, Beijing University of Chemical Technology, China Ministry of Education, Beijing 100029, China

Received 15 May 2007; accepted 26 August 2007

DOI 10.1002/app.27337

Published online 20 March 2008 in Wiley InterScience (www.interscience.wiley.com).

ABSTRACT: In this article, a new nitrile-butadiene rubber (NBR) crosslinked composites containing poly(vinyl chloride) (PVC) and hindered phenol (AO-80 and AO-60) was successfully prepared by melt-blending procedure. Microstructure and dynamic mechanical properties of the composites were investigated using SEM, DSC, XRD, and DMTA. Most of hindered phenol was dissolved in the NBR/PVC matrix and formed a much fine dispersion. The results of DSC and DMTA showed that strong intermolecular interaction was formed between the hindered phenol and NBR/PVC matrix. The NBR/PVC/AO-80 crosslinked composites showed only one transition with higher glass transition temperature and higher $\tan \delta$ value than the

neat matrix, whereas for the NBR/PVC/AO-60 crosslinked composites, a new transition appeared above the glass transition temperature of matrix, which was associated with the intermolecular interaction between AO-60 and PVC component of the matrix. Both AO-80 and AO-60 in the crosslinked composites existed in amorphous form. Furthermore, the chemical crosslinking of composites resulted in better properties of the materials, e.g., considerable tensile strength and applied elastic reversion. © 2008 Wiley Periodicals, Inc. *J Appl Polym Sci* 109: 106–114, 2008

Key words: hindered phenol; intermolecular interaction; dynamic mechanical properties; damping

INTRODUCTION

Rubber materials with low-frequency vibration and sound waves damping in the sonic and ultrasonic ranges are finding numerous applications, especially in the aircraft, automobile, and appliance industries. Based on the damping theory,^{1,2} the damping properties can be determined by dynamic mechanical behavior. The loss tangent $\tan \delta$ and the loss modulus E'' are measures of the damping that requires transformation the mechanical energy into heat. The damping properties of rubber materials are dominated by the glass transition, usually, the useful damping temperature range is about 20–30°C around the glass transition temperature. Some methods could be used to modify the dynamical properties of rubber, such as the interpenetrating polymer network blend and copolymerization.^{3–10} But all of these methods could not obtain a damping material with a high $\tan \delta$ value and a wide temperature rang at the same time. Wang et al. developed a new gradient polymer with a wide damping temperature range by *in situ* chemical modi-

fication of rubber during vulcanization. This gradient polymer exhibited a wide transition temperature range over 100°C with a peak half width of 69°C.¹¹

During recent years, some studies have been devoted to organic hybrids consisting of polar polymers and small organic molecules because of their special properties.^{12–15} Pioneered research conducted by Wu et al. revealed that, as compared to the neat rubbers (e.g., chlorinated polyethylene CPE), the organic hybrids consisting of hindered phenol and thermoplastic elastomer could obtain much higher dynamic mechanical loss property.^{12–15} They considered that when the hindered phenol particles, such as AO-80, are abundantly mixed with CPE, a minority of the AO-80 seems to be dissolved into the CPE matrix, but most of the AO-80 forms domains composed of an AO-80-rich phase, including some CPE molecules. The intermolecular hydrogen bond was formed between the α -hydrogen of CPE and the hydroxyl group of AO-80 in this domain. As a result, a new transition appeared above the glass transition of CPE matrix, which was assigned to the dissociation of the intermolecular hydrogen bond.

However, CPE and acrylic rubber (ACM) were the only two polymers studied in this field by researchers at present.^{11,13} Moreover, previous studies did not chemically crosslink these rubber hybrids, which

Correspondence to: L.-Q. Zhang (zhanglq@mail.buct.edu.cn).

would be possibly harmful to the tensile strength and elastic recovery property, especially for ACM. And also, no tensile properties were reported in references.

In this research, the compound of nitrile-butadiene rubber (NBR) and poly(vinyl chloride) (PVC) (the blend ratio is 70 : 30, wt %) was selected to prepare the crosslinked rubber composites with two kind of hindered phenol : 3,9-bis[1,1-dimethyl-2[b-(3-tert-butyl-4-hydroxy-5-methylphenyl)propionyloxy]ethyl]-2,4,8,10-tetraoxaspiro[5,5]-undecane (AO-80) and tetrakis [methylene-3-(3-5-ditert-butyl-4-hydroxy phenyl)propionyloxy]methane (AO-60), respectively. As compared to CPE, the nitrile group in NBR has stronger polarity than the chlorine/carbon and -hydrogen/carbon bonds in CPE, and the polarity of the PVC molecule is also stronger than CPE. That is to say the matrix of NBR/PVC could form stronger intermolecular interaction with hindered phenol compared to CPE, and these will endow the NBR/PVC/hindered phenol composites good damping properties. Moreover, crosslinking was first introduced into the rubber/hindered phenol composites, which would greatly improve the tensile strength and elastic recovery property. Such a material design pushes rubber/hindered phenol composites into a more applied stage.

EXPERIMENTAL

Materials

NBR/PVC compound (the blend ratio is 70 : 30 and the Mooney viscosity is 70) was produced by Taiwan Nantex Chemical Industry Co., with a acrylonitrile weight percentage of 33% in NBR, which was abbreviated as NBVC in this article. AO-80 powder (ADK STAB) with the chemical purity was obtained from Asahi Denka Co. (Tokyo, Japan). AO-60 power was obtained from Beijing Additive Research Institute (Beijing, China), and the purity is 99.6%. Figure 1 is the chemical structure of AO-80 and AO-60. After the as-received AO-80/AO-60 was heated to 160°C and quickly quenched in liquid nitrogen, the quenched AO-80/AO-60 was obtained with the glass transition temperature of 40.9°C and 46°C, respectively, which was used as comparison sample in this article. Other chemicals and ingredients were purchased in China. All materials were used without further purification.

Sample preparation

NBVC/hindered phenol composites were prepared using the following procedures: (1) After NBVC was kneaded on a two-roll mill for 3 min at room temperature, hindered phenol was added with the NBVC/hindered phenol ratios of 100/0, 100/10, 100/30, 100/50, and 100/70; subsequently, the mixtures were

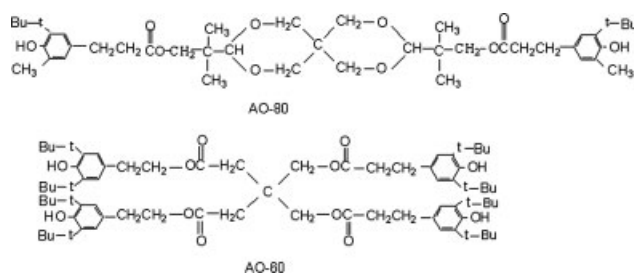


Figure 1 Chemical structure of AO-80 and AO-60.

blended at room temperature for 5 min to obtain the first-step NBVC/hindered phenol composites (which were termed as NBVC/hindered phenol-a composites). (2) NBVC/hindered phenol-a composites were directly kneaded on the two-roll mill for 5 min at 135°C (the temperature was higher than the melting point of AO-80 and AO-60) and cooled off at room temperature to obtain NBVC/hindered phenol-b composites. (3) After the NBVC/hindered phenol-b composites being cooled off, they were further mixed with crosslinking/compounding additives and blended on the two-roll mill at the room temperature for 10 min. (4) The mixture samples were finally hot-pressed and vulcanized at 160°C on an electrically heated hydraulic press with 15 MPa pressure for their optimum cure times (i.e., t_{90}) determined by a disc rheometer (P355C2, Beijing Huanfeng Chemical Technology and Experimental Machine Plant, China) to obtain NBVC/hindered phenol-c crosslinked composites.

In the composites, the recipe was 100 phr (parts per hundred of rubber by weight) NBVC, 5.0 phr zinc oxide, 2.0 phr stearic acid, 1.0 phr dibenzothiazole disulfide, 0.5 phr tetramethylthiuram disulfide, 2.0 phr sulfur, variable AO-80 and AO-60.

Analysis and characterization

Morphological, structural, and mechanical properties of the prepared NBVC/hindered phenol composites (including NBVC/hindered phenol-a, NBVC/hindered phenol-b, and NBVC/hindered phenol-c composites) were characterized using the instrumentation of SEM, DSC, XRD, DMTA, and tensile tester. The SEM images were taken from the representative fracture surfaces of the NBVC/AO-80 composites, using a XL-30 field emission ESEM made by FEI company in USA. The SEM specimens were prepared by fracturing the composites in liquid nitrogen. DSC measurements were performed with a DSC 204F1 calorimeter made by Netzsch Company in Germany. The DSC curves were recorded from -60 to 150°C at a heating rate of 10°C/min. XRD data were acquired from a Rigaku D/Max 2500VBZt/PC X-ray diffrac-

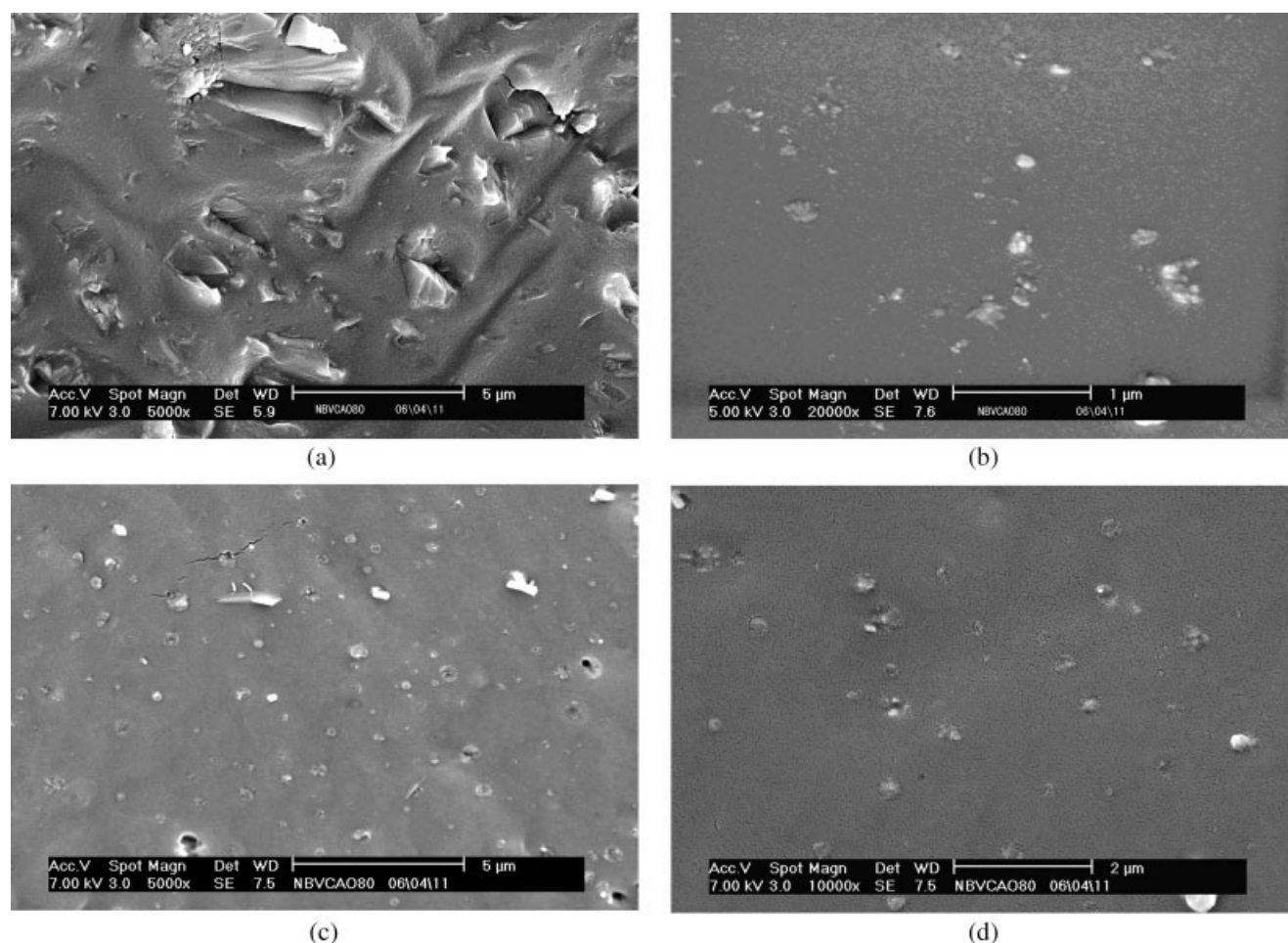


Figure 2 SEM images of the NBVC/AO-80(100/50) composites. (a) and (b) were NBVC/AO-80a(100/50) and NBVC/AO-80b(100/50), respectively; (c) and (d) were NBVC/AO-80c(100/50).

tometer Rigaku Corporation in Japan. The XRD data were recorded in the diffraction angle range of 3–30°.

Dynamic mechanical properties were carried out with a Dynamic Mechanical Thermal Analyzer (Rheometric Scientific DMTA) made by Rheometric Scientific Co. (New Jersey). The dimensions of the DMTA samples were 20-mm long, 6-mm wide, and 1-mm thick. The temperature dependence of the dynamic tensile module was measured in the range between –60 and 150°C, with the frequency of 1 Hz and the heating rate of 3°C/min. Tensile tests were conducted according to ASTM D 412. Dumbbell-shaped specimens of the NBVC/AO-80 composites were tested on a LRX plus Tensile Tester made by Lloyd Instruments (UK).

RESULTS AND DISCUSSION

NBVC/AO-80 crosslinking composites

Morphology of NBVC/AO-80 crosslinking composites

The representative SEM images of the prepared composites of the NBVC/AO-80(100/50) were shown in

Figure 2. First, it is clearly indicated that the normal mechanical blending of AO-80 and NBVC at the room temperature will lead to poor dispersion of AO-80 in the NBVC matrix, as so many big AO-80 particles (i.e., in the size of micrometers) could be observed in Figure 2(a). Besides, the interfacial adhesion between AO-80 particles and NBVC matrix was very weak, indicated by numerous holes due to the removal of AO-80 particles from the fracture surface. However, after NBVC/AO-80a(100/50) composite was kneaded on the two-roll mill for 5 min at 135°C (higher than the melting point of AO-80), as shown in Figure 2(b), the number and the average size of the dispersed AO-80 particles greatly decreased in the composite, which was termed as NBVC/AO-80b(100/50). During the kneading at 135°C, AO-80 particles melted into liquid form and then the liquid AO-80 could be easily dissolved into the polymer matrix, and so it is quite expectable that the original AO-80 particles had been dissolved in the matrix. Consequently, it would be more likely to allow AO-80 molecules to form strong interaction with the polar group in the matrix and also greatly reduced the cohesive energy of AO-80

during dispersing; as a result, a much fine dispersion was formed. And then, a few of AO-80 separated out from the matrix to form the submicron size particles during the following cool procedure, probably because the solubility of AO-80 in the matrix decreased at lower temperature, as also shown in Figure 2(b). During the following vulcanization process, the AO-80 molecules would diffuse into matrix from the AO-80 particles and the particle size decreased for that matter. On the other hand, the NBVC/AO-80c(100/50) composite formed a three-dimensional rubbery network, which could greatly depress the dissolvability of AO-80 molecules in the matrix. Consequently, the self-aggregation of AO-80 molecules was promoted, which resulted in the *in situ* generation of the particles. But with the degree of vulcanization increased, the reaggregation would be restricted by crosslinking network, so that the size of the reaggregation AO-80 particles were much smaller than that in NBVC/AO-80b(100/50).

The final dispersion structure of NBVC/AO-80c(100/50) was much fine, as illustrated in Figure 2(c): most AO-80 was dissolved in the matrix, and the partial was dispersed with the average size from tens of nanometer to 0.3 μm . The bright bigger particles in Figure 2(c) were the ZnO proved by element analysis attached with SEM, which was the one component of sulfur curing system. Figure 2(d) was the high magnification image of a small area in Figure 2(c).

Crystallization and glass transition of NBVC/AO-80 crosslinking composites

Figure 3(a) showed the DSC curves of the prepared NBVC/AO-80(100/50) composites. The DSC curves of AO-80 and unvulcanized NBVC were also included for comparison. As shown in Figure 3(a), the as-received AO-80 powder had the melting temperature around 122°C, and the unvulcanized NBVC had the glass transition temperature around -23.4°C (the endothermic peak around 90°C is associated with the microcrystalline PVC in the blends^{16,17}). Compared with the as-received AO-80, the quenched AO-80 did not display any melting peak around 122°C, indicating the polymorphous nature of AO-80. The NBVC/AO-80a(100/50) composite displayed both melting peak and glass transition characteristics, indicating that AO-80 and NBVC in the composite were not mixed well, which was consistent with the SEM results [Fig. 2(a)]. The early start of melting and the blunting of melting peak of AO-80 in the NBVC/AO-80a(100/50) composite suggested that the dissolving of AO-80 in matrix could happen with the increase in temperature during DSC measurement. However, in the NBVC/AO-80b(100/50) composite, the glass transition temperature of NBVC obviously shifted from -23.4°C to 0.1°C and the melting peak of AO-80 dis-

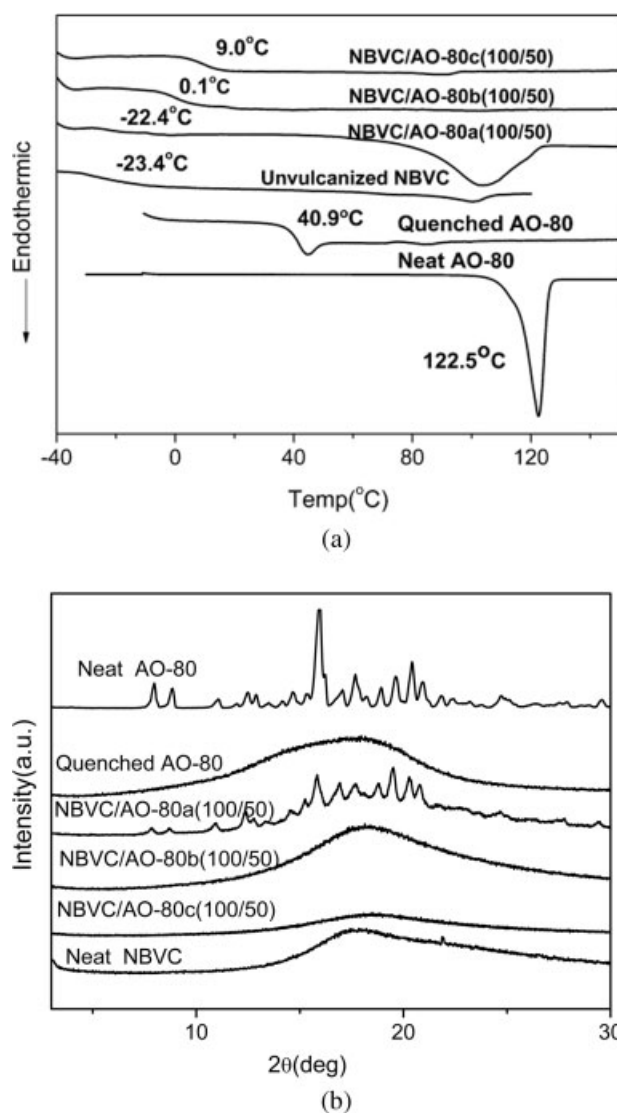


Figure 3 DSC (a) and XRD (b) curves of NBVC/AO-80(100/50) composites as well as quenched AO-80, neat AO-80, and NBVC.

appeared, which implied that AO-80 could be in an amorphous state or much finely dispersed in the matrix; moreover, a strong intermolecular interaction between AO-80 and matrix could result. Since the T_g of AO-80 was not observed, combining the SEM results, the hypothesis of fine dispersion should be approved. As aforementioned, when the composite was kneaded at 135°C, AO-80 melted, and was likely to form strong intermolecular interaction with NBVC matrix. The strong intermolecular interaction acted as physical crosslinking points and remarkably restricted the mobility of matrix macromolecules, which greatly improved the glass transition temperature of NBVC. At the same time, during the subsequent cooling, the AO-80 molecules could not reaggregate and crystallize, mainly because of the strong intermolecular interaction and partly because of the fast cooling

rate. As a result, the AO-80 melting peak disappeared. After the NBVC/AO-80b(100/50) composite further underwent hot-pressing and crosslinking process to give the NBVC/AO-80c(100/50) crosslinked composite, the DSC curve showed little difference, except that the glass transition temperature of NBVC was further increased by 9° due to the chemical crosslinking.

Figure 3(b) showed the X-ray diffraction patterns of the prepared NBVC/AO-80(100/50) composites as well as the neat AO-80, quenched AO-80, and NBVC matrix. The as-received and quenched AO-80 displayed typical crystalline and amorphous characteristic, respectively. The diffraction pattern of the NBVC/AO-80a(100/50) composite was similar to that of the neat AO-80, indicating that the AO-80 in the NBVC/AO-80a(100/50) composite was in crystalline form. However, the diffraction patterns of NBVC/AO-80b(100/50) and NBVC/AO-80c(100/50) indicated that AO-80 in both composites were amorphous. The XRD results were consistent with the DSC results, and further supported the aforesaid discussions.

Dynamic mechanical property of NBVC/AO-80 crosslinking composites

The loss tangent $\tan \delta$ is the crucial measure of the damping property of materials. The temperature dependence of the loss tangent ($\tan \delta$) values of the prepared NBVC/AO-80c crosslinked composites with various mass ratios of NBVC/AO-80 was shown in Figure 4. It was different from the CPE/AO-80 composites in previous work,¹² and every single composite had only one $\tan \delta$ peak, which was corresponding to the glass transition of the composites. This characteristic is consistent with that expressed by DSC. Furthermore, the $\tan \delta$ peaks shifted to higher tempera-

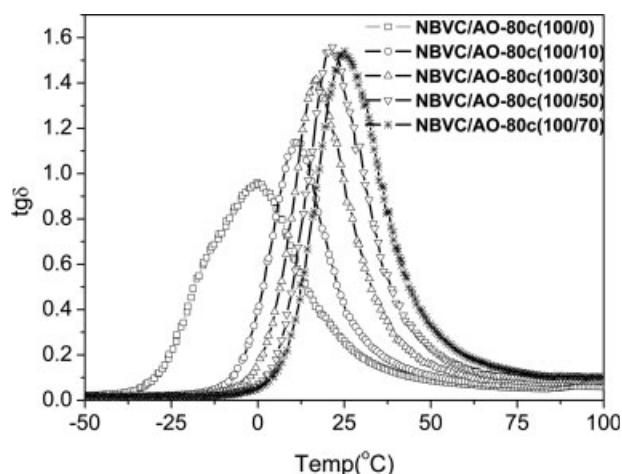


Figure 4 Temperature dependence of the loss tangent values for NBVC and NBVC/AO-80c crosslinked composites.

tures with increase in AO-80 amount in the composites. This result once again supported that, in the NBVC/AO-80c composites, the interaction between matrix and AO-80 was very strong, and the dispersion of AO-80 in the matrix was very fine, even at a very high ratio of AO-80 to NBVC matrix. The fine dispersion of AO-80 at the very high loading in return approved strong interaction between AO-80 and matrix, which limited the phase separation.

More importantly, with increase in the AO-80 amount from 0 to 70 phr, peak values of the $\tan \delta$ of the NBVC/AO-80c crosslinked composites increased from 0.95 to 1.56, and the $\tan \delta$ peaks around the room temperature also became distinctly wider. Such uncommon increase of the $\tan \delta$ value was very interesting. As well investigated, the introduction of inorganic fillers^{18–20} (e.g., carbon black, silica, and metal oxide/hydroxide) or organic small molecules²¹ (which act as a plasticizer of a bulk polymer) into polymer matrix lead to a direct decrease of the $\tan \delta$ value because of the volume effect or plasticizing effect. In normal case, the interaction between the filler and the polymer chain is very weak. The decrease of polymer amount in the composites could directly affect the $\tan \delta$ value of the composites. For the NBVC/AO-80c crosslinked composites, however, the increase in $\tan \delta$ value could be attributed to the strong intermolecular interaction between the fine dispersed AO-80 molecules/particles and the rubber matrix, which effectively restricted the motion of rubber macromolecules and increased the intermolecular friction during dynamic deformation. The high energy dissipation of intermolecular interaction under dynamic deformation was responsible for the remarkable increase of $\tan \delta$ values. High $\tan \delta$ in glass transition region suggested that the NBVC/AO-80c composites could be a good damping material at the corresponding working temperature range.

The temperature dependence of the storage modulus E' of the NBVC/AO-80c crosslinked composites with various mass ratios of NBVC/AO-80 was shown in Figure 5. All the storage modulus curves displayed only one transition, which further proved the fine dispersion of AO-80 in the matrix. Based on our knowledge, in the case of inorganic fillers filled rubber composites, the E' value increased obviously as the content of the filler increased.¹⁸ But in the case of NBVC/AO-80c crosslinked composites, the E' value in the glassy region did not vary much as the content of AO-80 increased, whereas those in the rubbery region significantly decreased, leading to the increase of the relaxation strength. This could be explained as that the modulus of amorphous AO-80 particles was approximate to the crosslinked matrix, and so the AO-80 particles had little effect on the matrix's E' . In addition, the glass transition temperature of the amorphous AO-80 particles was about 40.9°C when

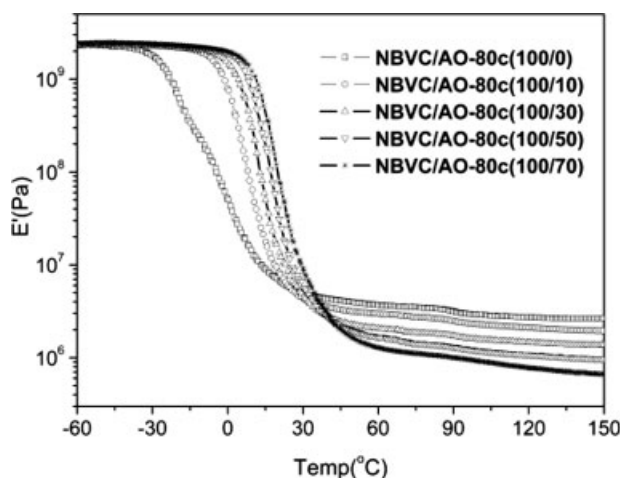


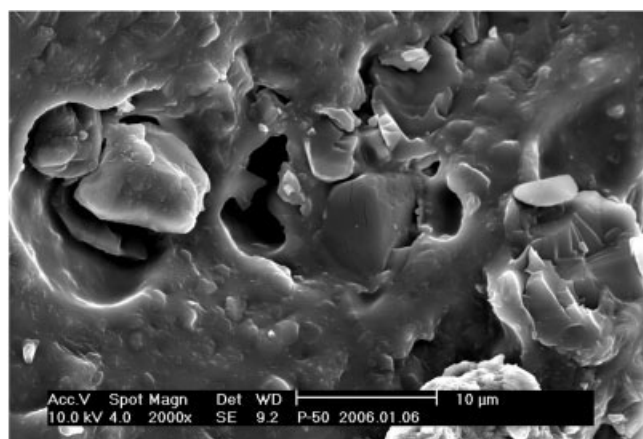
Figure 5 Temperature dependence of the storage modulus E' for NBVC and NBVC/AO-80c crosslinked composites.

the temperature exceeded this value, and the particles began to become soft and act as plasticizer, which decreased the E' value at the rubber region of NBVC/AO-80 crosslinked composites.

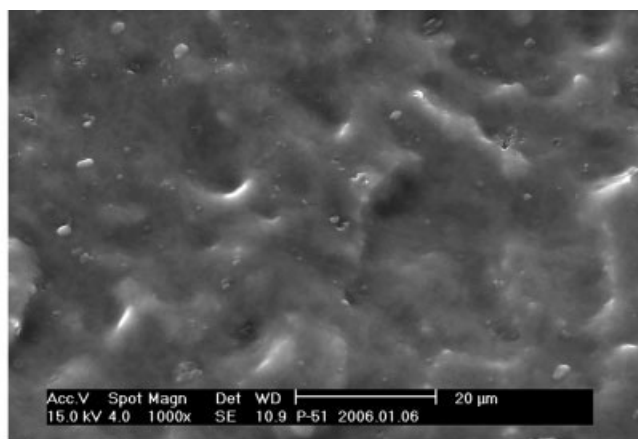
NBVC/AO-60 crosslinking composites

Morphology of NBVC/AO-60 crosslinking composites

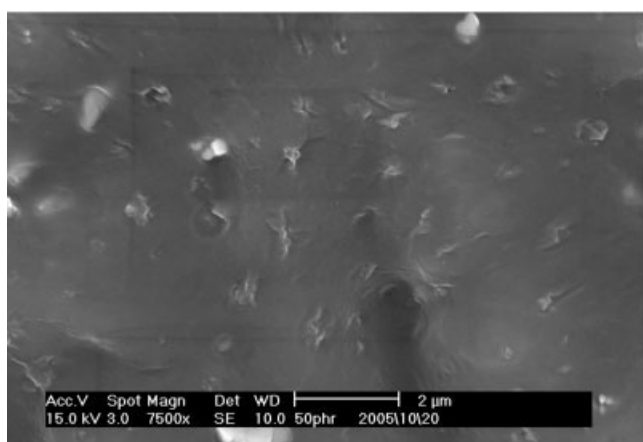
The morphology changes of the NBVC/AO-60(100/50) composite during the preparation process were shown in Figure 6. It was similar to the NBVC/AO-80(100/50) composite: in the NBVC/AO-60a (100/50), AO-60 was dispersed with the micron size in the NBVC matrix and the interfacial bonding of AO-60 particle/matrix was not strong; and then after the hot mixing process, AO-60 original particles were partly dissolved in the matrix, and the AO-60 that separated out from the matrix was dispersed as submicron particles. During vulcanization process, the size of remnant AO-60 particles further decreased to form the final dispersion structure in Figure 6(c,d) [the high magnification image of a small area in Fig. 6(c)]: partial AO-60 was dissolved in the matrix, and the other was dispersed with the size of 0.3–1 μm , which were bigger than the AO-80 particles in the NBVC/AO-80c(100/50) [Fig. 2(c,d)] owing to the lower compati-



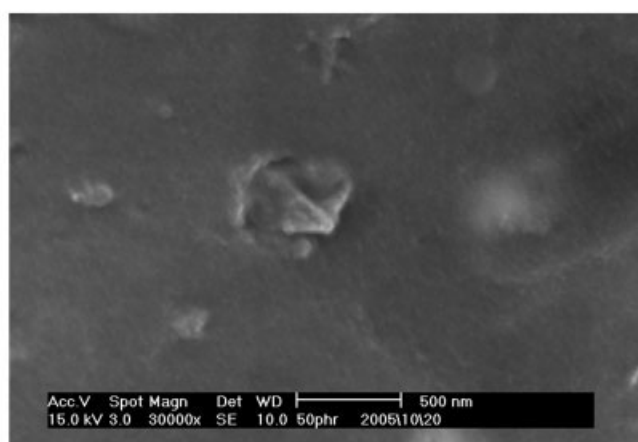
(a)



(b)



(c)



(d)

Figure 6 SEM images of the NBVC/AO-60(100/50) composites. (a) and (b) were NBVC/AO-60a(100/50) and NBVC/AO-60b(100/50), respectively; (c) and (d) were NBVC/AO-60c(100/50).

bility of AO-60 and matrix. Compared with the Figure 2(b-d), it was clearly found that the number of particles in the NBVC/AO-60 composites was much more than that in NBVC/AO-80 composites, indicating that less AO-60 was dissolved in the matrix owing to lower solubility of AO-60 in the matrix than that of AO-80.

Crystallization and glass transition of NBVC/AO-60 crosslinking composites

Figure 7 showed the DSC curves of the NBVC/AO-60c crosslinked composites; AO-60, quenched AO-60, and NBVC were also included for comparison. As shown in Figure 7, the as-received AO-60 powder had the melting temperature around 124°C, but the quenched AO-60 presented a glass transform at 46°C and the melting peak disappeared indicating the polymorphous nature of AO-60, which is similar to AO-80. However, after hot mixing with NBVC and then vulcanized, the melting peak of AO-60 disappeared, suggesting that AO-60 existed in amorphous form. Furthermore, the glass transition temperature of the composites increased with increase in AO-60 content, which is due to the intermolecular interaction between AO-60 and NBVC matrix. But the increasing magnitude of glass transition temperature of NBVC/AO-60 composites was much less than NBVC/AO-80 composites [Fig. 3(a)], because the intermolecular interaction was weaker than AO-80 composites.^{12,13}

Figure 8 showed the XRD curves of the NBVC/AO-60 composites as well as the quenched AO-60, neat AO-60, and NBVC matrix. The as-received and quenched AO-60 displayed typical crystalline and amorphous characteristic, respectively. The diffraction patterns of NBVC/AO-60 crosslinked composites indicated that AO-60 in each composite was amor-

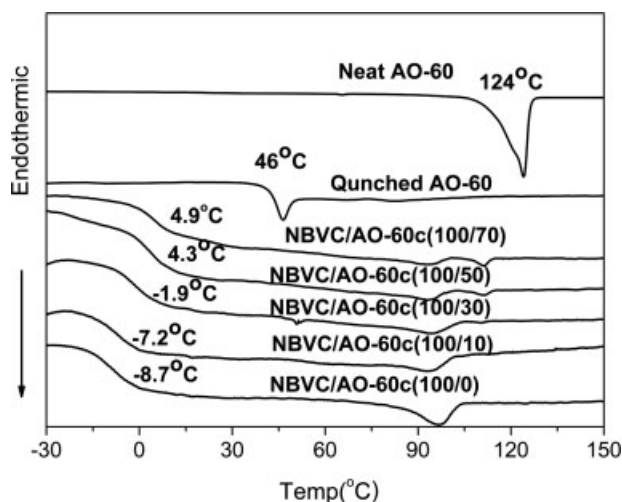


Figure 7 DSC curves of NBVC/AO-60c crosslinked composites as quenched AO-60, neat AO-60, and NBVC.

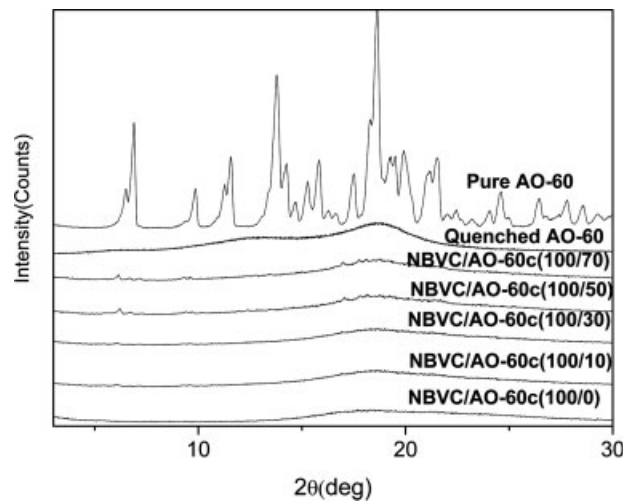


Figure 8 XRD curves of NBVC/AO-60c crosslinked composites as quenched AO-60, neat AO-60, and NBVC.

phous, which was consistent with the DSC results. Additionally, when the AO-60 loading was higher than 50 phr, there was a slender diffraction peak at $2\theta = 6^\circ$ and the diffraction strength slightly increased as the AO-60 content increased. It was due to the number of undissolved AO-60 particles increased in the matrix as the AO-60 content increased and the size of AO-60 particles in NBVC/AO-60c(100/50) were bigger compared with the lower AO-60 content crosslinked composites. Because the cool speed inside the larger particles was slower than the smaller ones, the AO-60 molecules in those larger particles had more time to rectify the molecules' conformation to form orderly structure. Therefore, we could assign the endothermic peaks around 110°C on the DSC curves of NBVC/AO-60c(100 : 50, 100 : 70), as shown in Figure 7, to this orderly structure of AO-60.¹³

Dynamic mechanical property of NBVC/AO-60 crosslinking composites

The temperature dependence of the loss tangent values ($\tan \delta$) of the prepared NBVC/AO-60c crosslinked composites with various mass ratios of NBVC/AO-60 was shown in Figure 9. As shown in Figure 9, the NBVC matrix had only one $\tan \delta$ peak; but after mixing with AO-60 (30, 50, and 70 phr), a new transition appeared above the glass transition temperature of the matrix. Furthermore, the $\tan \delta$ value of two transitions increased and the $\tan \delta$ position of the matrix shifted to higher temperature with increasing AO-60 content. As discussed in the NBVC/AO-80c crosslinking composites, the intermolecular interaction could prominently improve the $\tan \delta$ value of the matrix. Similarly, in the NBVC/AO-60 composites, the hydroxyl group of the AO-60 molecules formed intermolecular interaction with the

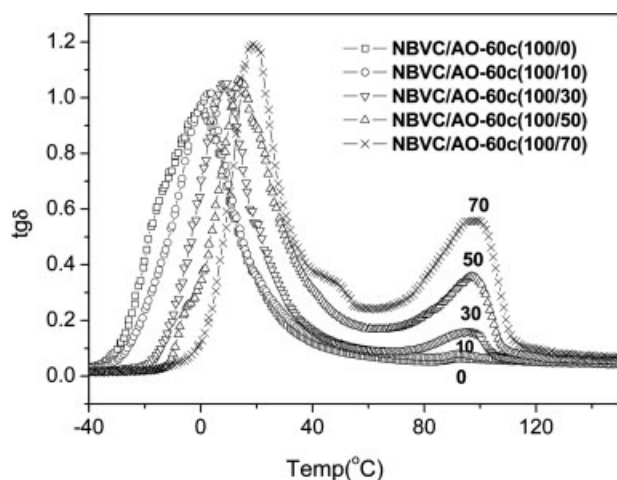


Figure 9 Temperature dependence of the loss tangent values for NBVC and NBVC/AO-60c crosslinked composites.

nitrile group of NBR, which acted as the physical crosslinked joints and improved the $\tan \delta$ value and the glass transition temperature of the cured NBR component. The new transition above the glass transition of temperature NBVC matrix in the NBVC/AO-60 crosslinking composites was caused by the intermolecular interaction between the hydroxyl group of the AO-60 and the chlorine of PVC. Compared with the AO-80 composites, the reason for appearance of this new transition in AO-60 composites could be explained by the steric effect of the bigger AO-60 molecules. As shown in Figure 1, there were two *tert*-butyl groups beside the hydroxyl group in AO-60 molecules, while there was only one *tert*-butyl group and a small methyl group near the hydroxyl group of AO-80. Moreover, the volume of the chlorine in PVC was smaller than that of the nitrile group in NBR. As a result, the chlorine of PVC would interact more easily with the hydroxyl group of AO-60 to form intermolecular interaction in the NBVC/AO-60 composites. But when the loading of AO-60 was lower than 10 phr in the NBVC/AO-60 composites, it would preferentially be dispersed in the NBR component, because the volume percentage of NBR was much higher than PVC component. It was the reason why the NBVC/AO-60(100/10) composite did not markedly show the new transition. But when the AO-60 content was higher than 10 phr in the composites, the contact between AO-60 and PVC molecules increased, and so the intermolecular interaction between PVC and AO-60 was enhanced.

Compared with Figures 4 and 9, it is quite expectable that the intermolecular interaction primary formed between AO-80 and NBR component in the NBVC/AO-80 crosslinked composites, while in the NBVC/AO-60 crosslinked composites, the interaction between AO-60 and PVC component acted important

effect as well as the interaction between AO-60 and NBR component.

Figure 10 showed the temperature dependence of the storage modulus E' of the NBVC/AO-60c crosslinked composites. Different from NBVC/AO-80c composites, the E' curves of NBVC/AO-60c composites showed two transitions region and three plateau regions. The first transition was associated with the glass transition of the rubber matrix and the transition temperature increased with the increase in AO-60 content, as discussed in the DSC curves (Fig. 7). The second transition was assigned to the dissociation of the in intermolecular interaction between PVC and AO-60. The E' in intermediate plateau was amplified in the top right corner of Figure 10. It was clearly showed that the E' value of NBVC/AO-60c (100/10) was lower than the neat matrix; but when the AO-60 content was higher than 10 phr, the E' of NBVC/AO-60c increased continuously in respect that the intermolecular interaction between PVC and AO-60 was enhanced.

Static mechanical property of NBVC/hindered phenol(AO-60,AO-80) crosslinked composites

The mechanical properties of the NBVC/AO-60c and NBVC/AO-80c crosslinked composites were summarized in Table I. The unvulcanized NBVC/AO-80b(100/50) composite which could not be used practically exhibited low tensile strength and high permanent set. But after curing, the tensile strength of NBVC/AO-60c and AO-80c crosslinked composites was much improved, and as indicated by NBVC/AO-80(100/50), the tensile strength of the vulcanized composites was much higher than that of unvulcanized one. Additionally, at the same loading of hindered phenol, the maximum strength of NBVC/AO-

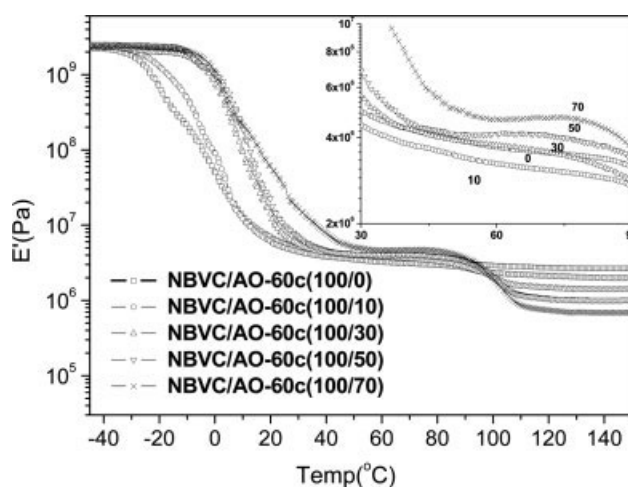


Figure 10 Temperature dependence of the storage modulus E' for NBVC and NBVC/AO-60c crosslinked composites.

TABLE I
The Mechanical Properties of NBVC/AO-60c and NBVC AO-80c Crosslinked

Properties	Loading of AO-60 (phr)					Loading of AO-80 (phr)				
	0	10	30	50	70	10	30	50	70	50 ^a
Hardness (Shore A)	75	83	90	94	95	85	93	95	95	–
Tensile strength (MPa)	10.7	14.3	15.1	15.1	10.2	12	14.7	17.8	19.9	4.5
Elongation at break (%)	366	364	403	402	385	399	458	462	476	1000
Permanent set (%)	6	8	12	28	44	8	12	24	36	>100

^a Unvulcanized NBVC/AO-80 b (100/50) composite.

80c composites was much higher than that of NBVC/AO-60c composites for the reason that the intermolecular interaction in NBVC/AO-80c composites was stronger than that in NBVC/AO-60c composites. Moreover, it clearly indicated in Table I that the NBVC/hindered phenol crosslinked composites had a small permanent residual deformation and could be used in industry in most cases, especially for NBVC/AO-80c composites.

CONCLUSIONS

A new rubber crosslinked composite containing hindered phenol (AO-80 and AO-60) was successfully prepared by melt-blending procedure. In the NBVC/AO-80c crosslinking composites, most AO-80 dissolved in the NBVC matrix and formed strong intermolecular interaction with NBR of the matrix. All the NBVC/AO-80c crosslinked composites had only one $\tan \delta$ peak. Furthermore, the $\tan \delta$ peaks shifted to higher temperatures and the $\tan \delta$ value increased with increase in AO-80 amount in the composites. But in the NBVC/AO-60c composites, because most of the AO-60 had formed intermolecular interaction with the PVC component of the matrix, a new transition appeared above the glass transition temperature of the matrix, and the $\tan \delta$ value of this novel transition increased with the increase in AO-60 loading. Both AO-80 and AO-60 in the crosslinked composites existed in amorphous form. As expected, curing had significant effect on improving the tensile strength and other mechanical properties of the NBR/PVC/hindered phenol composites. All the crosslinked NBVC/hindered phenol showed considerable tensile strength and very low permanent set. The NBVC/

hindered phenol crosslinked composites could be used as good damping materials.

References

- Sperling, L. H.; Fay, J. J. *Polym Adv Technol* 1991, 2, 49.
- Fradkin, D. G.; Foster, J. N.; Thomas, D. A.; Sperling, L. H. *Polym Eng Sci* 1986, 26, 730.
- Manoj, N. R.; Ratna, D.; Dalvi, V.; Chandrasekhar, L.; Patri, M.; Chakrabom, B. C.; Deb, P. C. *Polym Eng Sci* 2002, 42, 1748.
- Mathew, A.; Groeniecekx, G.; Michler, G. H.; Radusch, H. J.; Thomas, S. J. *Polym Sci B: Polym Phys* 2003, 41, 1680.
- Chern, Y. C.; Tswng, S. M.; Hsieh, K. H. *J Appl Polym Sci* 1999, 74, 328.
- Manoj, N. R.; Chandrasekhar, L.; Patri, M.; Chakraborty, B. C.; Deb, P. C. *Polym Adv Technol* 2002, 13, 644.
- Perera, M. C. S.; Ishak, Z. A. M. *Eur Polym J* 2001, 37, 167.
- Yamada, N.; Shoji, S.; Sasaki, H.; Nagatani, A.; Yamaguchi, K.; Kohjiya, S.; Hashim, A. S. *J Appl Polym Sci* 1999, 71, 855.
- Qin, C. L.; Cai, W. M.; Cai, J.; Tang, D. Y.; Zhang, J. S. *Mater Chem Phys* 2004, 85, 402.
- Chu, H. H.; Lee, C. M.; Huang, W. G. *J Appl Polym Sci* 2004, 91, 1396.
- Wang, Y. Q.; Wang, Y.; Zhang, H. F.; Zhang, L. Q. *Macromol Rapid Commun* 2006, 27, 1162.
- Wu, C. F.; Yamagishi, T.; Nakamoto, Y.; Ishida, S.; Nitta, K.; Kubota, S. *J Polym Sci Part B: Polym Phys* 2000, 38, 2285.
- Wu, C. F.; Yamagishi, T.; Nakamoto, Y.; Ishida, S.; Nitta, K.; Kubota, S. *J Polym Sci Part B: Polym Phys* 2000, 38, 1496.
- Wu, C. F. *J Appl Polym Sci* 2001, 80, 2468.
- Wu, C. F.; Otani, Y. *J Appl Polym Sci* 2001, 82, 1788.
- Dawson, P. C.; Gilbert, M. J. *Polym Sci Part B: Polym Phys Ed* 1991, 29, 1407.
- Huang, Z. M.; Bao, Y. Z. *Polym Mater Sci Eng* 1999, 15, 10.
- Pattanawanidchai, S.; Saeoui, P.; Sirisinha, C. *J Appl Polym Sci* 2005, 96, 2218.
- Sirisinha, C.; Prayoonchatphan, N. *J Appl Polym Sci* 2001, 81, 3198.
- Bazgir, S.; Katbab, A. A.; Nazockdast, H. *J Appl Polym Sci* 2004, 92, 200.
- Kalkar, A. K.; Parkhi, P. S. *J Appl Polym Sci* 1995, 57, 233.